Durability and leach-ability evaluation of K-based geopolymer concrete in real environmental conditions

Peiman Azarsa, & Rishi Gupta

April 2020

Case Studies in Construction Materials 13 (2020) e00366

Contents lists available at ScienceDirect

Case Studies in Construction Materials

journal homepage: www.elsevier.com/locate/cscm

Case study

Durability and leach-ability evaluation of K-based geopolymer concrete in real environmental conditions

Peiman Azarsa[a], Rishi Gupta[b,*,1]

[a] Department of Civil Engineering, University of Victoria, Victoria, Canada
[b] Department of Civil Engineering, University of Victoria, Victoria, Canada

ARTICLE INFO

Article history:
Received 19 August 2019
Received in revised form 20 April 2020
Accepted 21 April 2020

Keywords:
Real environmental exposure
Geopolymer concrete
Fly-ash
Bottom-ash
Potassium-based
Non-destructive tests
Durability
Leaching

ABSTRACT

Geopolymer Concrete (GPC) as an alternative to Portland Cement Concrete (PCC) is a cement-less and green construction material which is produced by mixing industrial by-products with an alkaline solution. In this study, PCC and Potassium-based (K-based) GPC synthesized with 50 % fly-ash and 50 % bottom-ash were exposed to the real environmental conditions to evaluate their chemical metals leach-ability and durability over 150 and 240 days of exposure respectively. The mix contained potassium hydroxide concentration of 12 molarity, potassium silicate/potassium hydroxide ratio of 1.47, alkaline solution/ashes (fly-ash and bottom-ash) ratio of 0.54 and total aggregate content of 1800 kg/m^3. To develop GPC, two methods of curing (steam curing and dry curing) were used to increase the compressive strength of GPC. According to the result of compression test, the compressive strength of steam-cured GPC increased 3.5 times when temperature elevated from ambient temperature (~10 °C) to 80 °C. While, an increase in compressive strength of dry-cured GPC samples was 2.3 times. Non-Destructive Tests (NDT)s including Schmidt hammer, ultrasonic pulse velocity and resonant frequency test were employed to measure the relative dynamic modulus of elasticity. In this study, paver block has been selected as an application since to the best of our knowledge, there is no work reported the effect of real environmental conditions on leach-ability and mechanical properties of K-based GPC paver blocks. Two areas were paved with a total of 150 GPC and 210 PCC paver blocks. The results of the NDTs in area 1 show that the average velocity and compressive strength of GPC decreased approximately 11.6 % and 23.4 % respectively. While, the average velocity and compressive strength of PCC decreased about 8.3 % and 8.2 % respectively. In area 2, the average rate of velocity and compressive strength loss of GPC was about 12.03 % and 19.51 % respectively. Whereas, maximum decrease in average velocity and compressive strength of PCC over 240 days of exposure was 5.28 % and 9.65 % respectively. Leach-ability of GPC as another innovative aspect of current study was also measured using HACH strips since the release of heavy metals can be a concern in GPC. The results indicate that due to the heat-treatment of GPC paver blocks, all the parameters including total alkalinity, total hardness, pH, total chlorine, phosphate, copper, ammonia, iron, nitrate and nitrite were within the standard domain and were constant over 150 days of exposure. The relative dynamic modulus of elasticity power function model and exponential function model were established to find a suitable damage predictive model for both types of concrete. It was concluded that due to the higher values of Adj.R^2 for both GPC (0.96) and PCC (0.92), the power function relationship compared well with the exponential function.

* Corresponding author at: Department of Civil Engineering, University of Victoria, Victoria, Canada.
E-mail addresses: azarsap@uvic.ca (P. Azarsa), guptar@uvic.ca (R. Gupta).
[1] Postal address: ECS building, Civil engineering department, University of Victoria, 3800 Finnerty Rd, Victoria, BC V8P 5C2.

https://doi.org/10.1016/j.cscm.2020.e00366

1. Introduction

In the past few decades, emission of Carbon Dioxide (CO_2) through human and natural processes such as human activities, disposal of waste materials and consuming natural resources is considered as the most important cause of climate change. In the construction industry, cement production is one of the main contributors to increasing CO_2 emission in the world. That is why the utilization of waste material in the production of concrete can be a possible alternative to cement [1]. According to Mohammadhosseini et al. [2] and Dimitriou et al. [3], greater utilization of waste materials mitigate the negative environmental impacts. Since waste materials are used in numerous applications, it is essential to investigate their effect on the mechanical properties of materials produced. The study by Mohammadhosseini et al. [4] shows that the mechanical properties of Self-Compacting Concrete (SCC) including compressive strength, splitting tensile and flexural strength can be improved by water/binder ratio of 0.4 and 30 % replacement of palm oil fuel ash with cement.

Toward achieving a sustainable material and green environment, Geopolymer Concrete (GPC) has been materialized as one of the alternatives to Portland Cement Concrete (PCC) in the construction industry due to its ability to minimize the requirement for natural resources. GPC uses natural aluminosilicate materials activated by an alkali activator, which are then combined with fine and coarse aggregates. Moreover, previous studies [5,6] on GPC indicate that it can be used for the construction applications due to sufficient durability, workable slump, and comparable grade of strength to its counterpart PCC. The studies by Hardjasaputra et al. [7] and Zerzouri et al. [8] indicate that GPC offers considerable durability and mechanical properties compared to conventional concrete including compressive strength, flexural strength, elastic modulus, sulfuric acid attack resistance etc. Pereira et al. [9] pointed out that both GPC and PCC achieved similar compressive strength (≒ 60 MPa) upto 2 years of ageing. In addition, Nabeel et al. [10] reported that GPC synthesized by fly-ash and slag had lower Ultrasonic Pulse Velocity (UPV) than Ordinary Portland Cement (OPC). However, Nabeel et al. [10] also mentioned that both GPC and OPC with UPV range of 3.5–4.5 K m/s are categorized as "good" quality concrete at age of 7 days and 28 days.

Fly-ash is one of the main constituents of GPC that is pulverized and blown with air into the furnace where it ignites, generates heat and forms ash. Fly-ash is a pozzolan material, containing aluminous and siliceous which forms a compound similar to cement. According to Abualrous et al. [11], the most effective line of attack to increase the waste materials amount in limited lands and reduce CO_2 emission is using fly-ash as a supplementary cementitious material or partial substitution for clinker production. It is reported that about 80 % of the unburned material or fly-ash is entrained in the flue gas when pulverized coal is burned in a dry condition. The remaining 20 % of the ash is dry bottom-ash that has similar chemical properties to fly-ash, consisting of silica and alumina [12]. However, often ignored, bottom-ash as part of the non-combustible residue of combustion in a furnace can also be used to produce a green construction material. That is why, in the current study, attempts have been made to produce GPC made by combination fly-ash and bottom-ash. Thaarrini and Ramasamy [13] reported that bottom-ash based GPC with Sodium Hydroxide (NaOH) and Sodium Silicate (Na_2SiO_3) ratio of 2 yielded a compressive strength of 41.53 MPa and 48.55 MPa under ambient and steam curing (60 °C) conditions respectively.

The utilization of fly-ash or bottom-ash to produce GPC requires an alkaline solution. The most common alkaline solutions used in GPC studies are NaOH and Na_2SiO_3 [14–18]. However, a few studies such as Sakkas et al. [19] as well as Hosan et al. [20] reported that the combination of alkaline solution such as Potassium Hydroxide (KOH) and soluble silicate such as Potassium Silicate (K_2SiO_3) can also be used in the production of GPC. Sabitha et al. [21] and Bakharev et al. [22] reported that although sodium-based activators are broadly used for the production of GPC, potassium-based activators are also claimed to decrease the initial setting, improve the geopolymerization process and consequently, increase the compressive strength of GPC as well as its workability. Therefore, in this study attempts have been made to develop a Potassium-Based (K-based) GPC using a unique combination of fly-ash and bottom-ash. Table 1 shows the flow of knowledge on the development of GPC.

1.1. Research significance

Since the consumption of bottom-ash is comparatively limited, utilizing this by-product material is one of the critical challenges in recent decades [23,24]. Hence, one of the main objectives of the current study is to develop a K-based GPC made by a combination of 50 % fly-ash and 50 % bottom-ash. Further, the knowledge gap on mechanical properties and leach-ability under real environmental exposure is filled. In this study, GPC paver block has been selected as an application since there is no work authors could find that reports the effect of low temperature and wetting-drying on K-based GPC's performance under real environmental conditions. As a laboratory investigation, Khandol et al. [25] pointed out that fly-ash based alkali activated paver block has superior compressive strength, abrasion resistance, and lower water absorption compared to its counterpart OPC.

Leaching assessment of GPC is another important concern and matter of interest in engineering concepts, which must be known when using this material in exposed applications. Numerous studies [26–28] have assessed the leach-ability of PCC, however, there is no information available for K-based GPC made by a combination of fly-ash and bottom-ash. Moreover, tests in real environmental conditions including cold climates to estimate the interaction of K-based GPC leaching with ground-water are not reported. Hence, another main objective of the present study is to investigate the leach-ability of chemical metals of both PCC and GPC over every thirty days of exposure. Izquierdo et al. [29] reported that fly-ash based geopolymer matrix is appropriate for the immobilization of many chemical elements including Be, Bi, Cd, Co, Cr, Cu, Nb, Ni, Pb, Sn, Th, U, Y, Zr. Though, the leaching amount of some elements such as B, Mo, Se, V were higher in the geopolymer matrix

Table 1
Flow of knowledge on the development of GPC.

References	Gaps/Findings
[1–3]	**Findings:** The use of waste materials in production of concrete reduce disposal of waste materials associated with CO_2 emission. **Gaps:** Small portion of waste materials was used in production of concrete. However, in the current study, attempts have been made to remove cement from the mixture and use waste materials in production of GPC.
[4]	**Gaps:** In this study [4], Palm Oil Fuel Ash (POFA) was used to enhance performance of the mixture. However, the effect of both fly-ash and bottom-ash on durability of GPC is still questioned. That is why in the current study, NDTs were employed to investigate durability of GPC made by both fly-ash and bottom-ash.
[5,6]	**Findings:** Both studies showed that GPC is a proper substitute to cement-based concrete which is environmentally friendly construction material. GPC uses low amount of natural resources, emits less CO_2 and has superior mechanical properties.
[7,8]	**Findings:** The investigation of various properties of GPC including elastic modulus, flexural strength and compressive strength etc. in both normal and aggressive conditions showed that GPC samples are slightly altered compared to its counterpart PCC.
[9,10]	**Gaps:** These two studies investigated mechanical properties of GPC made by fly-ash, slag and metakaolin. However, in the current study, attempts have been made to create a durable GPC made by fly-ash and bottom-ash. Moreover, authors could not find any research on mechanical properties of GPC made by fly-ash and bottom-ash in paver block application.
[11,12]	**Findings:** Based on the results, fly-ash can be used as a Pozzolan and fine aggregate in concrete. Moreover, this is the most sustainable approach to reducing the amount of fly-ash disposal. **Gaps:** These studies only compared different types of fly-ash in concrete. However, huge amount of bottom-ash is still disposed all over the world. That is why, the authors of the current study used bottom-ash as one of the main precursors of GPC.
[13]	**Findings:** This study showed that bottom-ash also can be used to produce a durable GPC with compressive strength range from about 11–49 MPa. **Gaps:** In the current study, the mechanical properties and durability of GPC paver blocks have been investigated in real environmental conditions and compared with its counterpart PCC paver blocks.
[14–22]	**Gaps:** It is well-known that Na-based solution is basically used in production of GPC. However, not much work reported on the mechanical properties of K-based GPC paver blocks in real environmental conditions. In the current study, NDTs such as UPV were used to investigate durability of K-based GPC paver blocks.
Contribution of this current study	As aforementioned, the mechanical properties and durability of fly-ash and bottom-ash in GPC have been explored by many researchers [1-22]. However, not much information is available on the durability and leaching of chemical metals of K-based GPC made by combination of 50% fly-ash and 50% bottom-ash in real environmental conditions association with real traffic load. That is why, this study creates a paradigm for future practical execution of this new generation of concrete called GPC.

as compared with fly ash (raw material). Several knowledge gaps that were indicated in this section are studied in this current work.

2. Precursors of GPC

2.1. Fly-ash and bottom-ash

In this study, class F fly-ash and bottom-ash were selected as fine particulate constituents of GPC to develop a sustainable concrete mix for constructing paver blocks. Based on ASTM C618 [30], three classes of fly-ash with various pozzolanic and cementitious properties are available. Generally, class F generated from burning anthracite or bituminous coal is used in the production of GPC. In this study, both fly-ash and bottom-ash were obtained from Lafarge Canada Inc.

According to a report made by Lafarge Inc., X-Ray Diffraction (XRD) was used to measure chemical elements of fly-ash and bottom-ash. Table 2 shows the comparison between chemical compositions of Lafarge fly-ash and other types of fly-ash from other sources. As can be seen in Table 2, all the available chemical elements of three types of fly-ash are in the range of ASTM C618 [30]. Comparing the chemical contents of three types of fly-ash, CaO was found in a greater percentage in Lafarge fly-ash which due to the polymerization reaction with hydrated materials results in a greater compressive strength [31].

Bottom-ash with coarser particle size compare to fly-ash was sieved (#1.18 mm) to remove large particles to increase the surface area of particle used to ultimately help to achieve reasonable strength. Table 4 shows the value of various chemical elements of three types of bottom-ash.

According to Table 2 and Table 4, the chemical compositions of both fly-ash and bottom-ash obtained from various sources are varied. It can be attributed to the chemical content of the coal burned and the type of operation process [34]. It

Table 2
Comparison between chemical compositions of Lafarge fly-ash and other types of fly-ash.

Properties	Fly-ash (%) Current study (Lafarge)	Fly-ash (%) [32]	Fly-ash (%) [33]	ASTM C618 (%) [30]
SiO_2	47.1	62.04	59.7	70 (min)
Al_2O_3	17.4	25.5	27.51	
Fe_2O_3	5.7	4.28	4.91	
CaO	14	3.96	1.45	N/A
MgO	5.4	1.27	1.18	N/A
SO_3	0.8	0.73	0.16	5.0 (max)
LOI	0.19	N/A	2.66	6.0 (max)
Na_2O	N/A	0.46	0.82	N/A
K_2O	N/A	N/A	2.39	N/A
TiO_2	N/A	1.33	N/A	N/A
P_2O_5	N/A	0.31	N/A	N/A
Mn_2O_3	N/A	N/A	N/A	N/A

The physical properties of fly-ash shown in Table 3 were analyzed at the Lafarge Seattle Concrete Lab. It can be seen in Table 3 that all the physical properties of used fly-ash in this study complies with the requirement of ASTM C618 [30].

Table 3
Physical properties of fly-ash.

	Fly-ash	ASTM C618 [30]
Fineness retained on 45 μm (No. 325 sieve)	17.3 %	< 34 % (complies)
Strength activity index with Portland cement % of control at 28 days	99 %	> 75 % (complies)
Water requirement, percent of control	100 %	< 105 % (complies)
Autoclave expansion	0.04 %	< 0.8 % (complies)
Density	2.65 Mg/m^3	< 5% (complies)

Table 4
Comparison between chemical compositions of Lafarge bottom-ash and other types of bottom-ash.

Properties	Bottom-ash (%) Current study (Lafarge)	Bottom-ash (%) [34]	Bottom-ash (%) [35]
SiO_2	60.11	22.90	19.12
Al_2O_3	14.35	0.18	12.03
Fe_2O_3	5.92	11.39	9.31
CaO	10.40	17.93	43.11
MgO	4.49	1.0.4	2.11
SO_3	0.10	0.73	2.39
LOI	0.00	N/A	N/A
Na_2O	2.232	3.68	2.35
K_2O	1.766	N/A	0.84
TiO_2	0.892	N/A	2.48
P_2O_5	0.200	N/A	2.62
Mn_2O_3	0.093	N/A	N/A

should be noted that there is no standard reported the specification/limitation for utilization of bottom-ash in a concrete mixture.

Table 5 shows the range of other properties of both fly-ash and bottom-ash obtained from the Material Safety Data Sheets (MSDS) of Lafarge Canada Inc. The physical properties of bottom-ash such as soundness are not precisely measured by Lafarge Canada Inc. because bottom-ash is not typically used in the construction industry.

The mix design shown in Table 6 was derived after initial trial experiments on mortars performed in the Facilities for Innovative Materials and Infrastructure Monitoring (FIMIM) by the authors [36–38]. Traffic is one of the most factors in paver block design. The deterioration caused to paver blocks by traffic depends on weight of the vehicles and number of load repetitions over the traffic analysis period. In order to quantify this deterioration, the number of Equivalent Single Axle Loads (ESAL) should be calculated. IS 15658 standard [39] recommended different grade of paver blocks for various construction areas and traffic categories. In accordance to IS 15658 standard [39], the grade of M35 (f'_C = 35 MPa) was considered for this study because less than 150 commercial vehicles daily used the parking area. The concentration of 12 Molarity (M) and 50:50 % mass ratio of bottom-ash to fly-ash were selected to achieve target strength of 35 MPa. This target strength was chosen to

Table 5
The range of other properties of both fly-ash and bottom-ash.

Material	Appearance	Odor	pH	Boiling point	Specific gravity	Solubility
Fly-ash	Gray/Black or Brown/Tan (Powder)	odorless	4–12	> 1000 °C	2.0–2.9 (water = 1)	Water: <5% (slightly)
Bottom-ash	Gray/Black or Brown/Tan (Powder)	odorless	4–12	> 1000 °C	2.0–2.9 (water = 1)	Water: <5% (slightly)

Table 6
Mix proportions of K-based GPC.

Material	Content (Kg/m^3)
Fly ash	194
Bottom ash	194
Coarse aggregates	1170
Sand	630
KOH (12 M)	85.16
K_2SiO_3	125.74
Extra Water	38.71
Air Entrained Admixture	1.5

produce GPC paver blocks with properties comparable to that of commercially available PCC paver blocks and to later compare the durability of these two types of paver blocks in real environmental conditions. However, the proprietary mix design of PCC paver blocks was not revealed by the manufacturer. Commercially produced PCC paver blocks were purchased from Abbotsford Concrete Products Manufacturer of Abbotsford, B.C., Canada.

2.1.1. Morphology of fly-ash and bottom-ash

A scanning Electron Microscope (SEM) was performed using Hitachi S-4800 to capture images of fly-ash and bottom-ash at the Advanced Microscopy Facility (AMF) of the University of Victoria. A thin layer of carbon was sputtered on the surface of ashes to increase the conductivity of particles. The SEM accelerating voltage of 15.0KV was used.

Basically, fly-ash particles are divided into three classes: solid sphere, cenospheres and plerospheres. Cenospheres fly-ash has lower bulk density, greater thermal resistance, higher workability and superior strength [40]. While, plerospheres are created by impregnated cenospheres with micro-spheres, which is why plerospheres are heavier than cenospheres due to extra weight of bagged microspheres [41].

As can be seen in Fig.1, fly-ash particles are glassy, spherical in shape and there is no evidence of cenospheres (totally hollow) and plerospheres (filled with several tiny spheres) shapes. Generally, lower fineness and low carbon content in fly-ash decrease the water demand of concrete [42] due to its specific surface role [43]. Table 2 shows that Loss of Ignition (LOI) of used fly-ash in the current study is 0.19 %. Fly-ash with less than 4% LOI is considered as low carbon content fly-ash. Fig. 1(a) & (b) present that all fly-ash particles are spherical glassy. The spherical glassy shape of fly-ash particles is also reported by Davidovits [44].

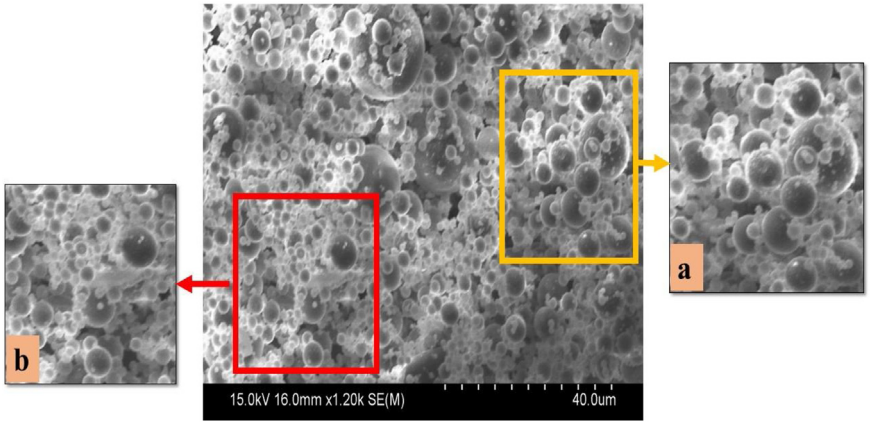

Fig. 1. SEM micrograph of fly-ash particles.
(a)& (b) Two random areas selected to characterize the shape of fly-ash particles.

A magnification of 1200x is used both in Figs. 1 and 2 for easy comparison. Based on these observations, it is expected that replacement of fly-ash with any amount of bottom-ash would negatively impact on workability, since not all bottom-ash particles were found to be spherical.

Fig. 2(a) and (b) were randomly selected to characterize the shape of bottom-ash particles. It can be seen that at the accelerating voltage of 15.0 KV, non-uniform shapes with a small amount of spherical shape were detected in bottom-ash samples.

In accordance to a previous study on microstructure of fly-ash and bottom-ash performed by the current authors [45], the particle size of fly-ash was about 1–20 μm with average size of 10 μm. While, the mean size of the rounded shape bottom-ash particles was 58.53 μm. The average height and width of the irregular shaped bottom-ash particles was 22.59 μm and 12.78 μm respectively.

2.2. Alkaline solution

As aforementioned, a combination of alkaline solution and soluble silicate is needed to begin the geopolymerization process. In this study, attempts have been made to improve the durability of GPC made by a combination of KOH and K_2SiO_3, as limited information is available on such type of GPC. The industrial grade KOH flakes obtained from Sigma-Aldrich Private Ltd, Canada was used in this work.

Potassium silicate powder (AgSil 16) obtained from PQ Corporation (USA) was used in this study. The chemical composition of K_2SiO_3 obtained from the MSDS of the product is shown in Table 7.

2.3. Aggregates

Fine aggregates and coarse aggregates were obtained from a quarry in British Columbia, Canada with a relative dry density of 2.67 and 2.71 respectively. The water absorption ratio of fine aggregates and coarse aggregates were 0.79 % and 0.69 % respectively. Fineness moduli of the coarse and fine aggregates were measured 6.85 and 3.54 respectively. The particle size distribution of coarse and fine aggregates were measured (shown in Fig. 3) in accordance with ASTM C33 [46].

3. Method of casting and curing

3.1. Specimen preparation

In this study, 300 GPC paver blocks were cast at the Civil Engineering Materials Facility at the University of Victoria in accordance with ASTM C192 [47].

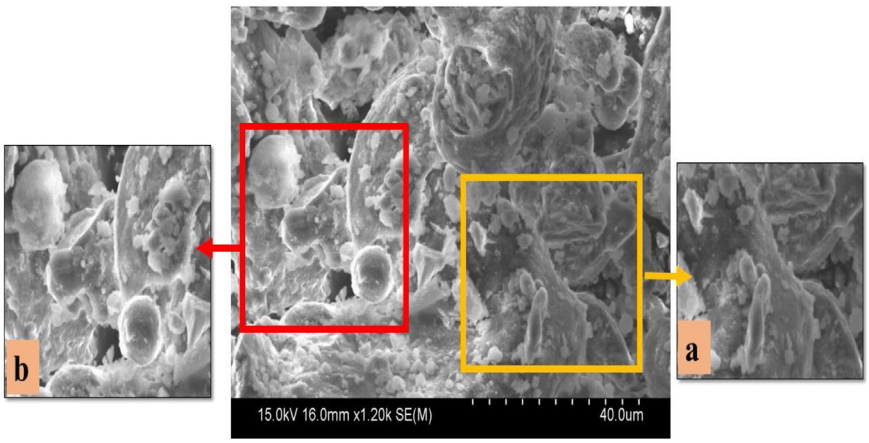

Fig. 2. SEM micrograph of bottom-ash particles.
(a) & (b) Two random areas selected to characterize the shape of bottom-ash particles.

Table 7
Chemical composition of K_2SiO_3.

Compound	K_2O	SiO_2	H_2O
%W/W	32.4 %	52.8 %	14.8 %

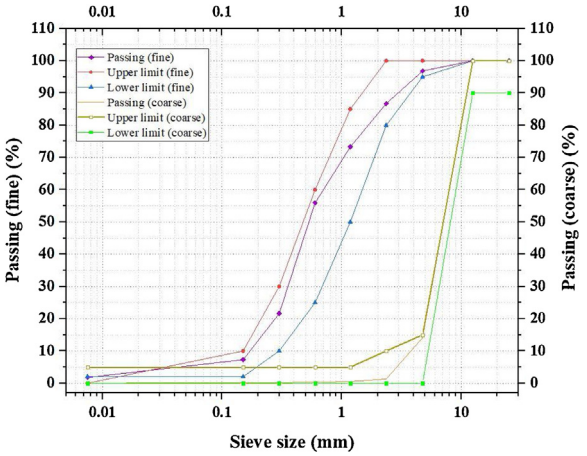

Fig. 3. Aggregates size distribution.

First of all, the KOH solution was prepared by mixing KOH flakes into water 24 h prior to the batching day. Secondly, sand and coarse aggregates were mixed for 30 s in dry condition. Ashes were added to aggregates and mixed for another 30 s. Solutions were then added to the dry materials and mixed until uniformity (~ 3 min), followed by a 3 min rest period, followed by 2 min of final mixing. The prepared material was placed into molds and vibrated using a table for 30 s to discharge air bubbles to the surface. After vibration, the molds were covered with a plastic sheet in the lab environment (approximate relative humidity range of 45 %–70 % and approximate temperature range of 5 °C–15 °C); and were demolded after 24 h.

3.2. Curing methods

Various trial mix designs were created to achieve a strength target of 35 MPa. Different curing temperatures and durations tested on cylindrical samples were selected to develop GPC since the curing temperature and duration is a critical parameter in the geopolymerization process to obtain higher strength. Two types of accelerated curing methods were used in this study:

3.2.1. Dry curing

Samples were kept in an oven at temperatures of 30, 45, 60, 80 °C for a period of 24 h followed by 24 h of ambient curing.

3.2.2. Steam curing

Half of the buckets were filled with water and then the samples were placed into the buckets. The buckets were sealed up to prevent excessive evaporation of water during the curing process and the samples were then kept into the oven at temperatures of 30, 45, 60, 80 °C. Authors refer to this curing regime as “steam curing” in this paper. Lastly, the paver blocks were removed after 24 h and were left at ambient temperature. Based on the results of the compressive strength test, steam curing at a temperature of 80 °C was chosen in the present research as the curing method.

Fig. 4(a) shows all the raw materials used in the production of GPC. Fig. 4(b) also shows the immersed paver block into water and cured at 80 °C to achieve higher compressive strength. Fig. 4(c) shows the cured paver block and Fig. 4(d) shows the size, color and shape of GPC after 28 days of curing.

4. Effect of geometry

Since the geometry of specimens affects the ultimate compressive strength of concrete [48,49], the compressive strength of cylindrical-shaped samples was compared to the compressive strength of rectangular-shaped samples (paver blocks) in accordance with British Standard EN-206 [50].

According to this standard, compressive strength test is performed on either 150 × 300 mm cylindrical or 150 mm cubical samples. As an example, when the minimum specified compressive strength of a cylindrical-shaped sample for lightweight concrete is 35 MPa, the cubic sample is expected to be 38 MPa [50]. However, it is mentioned in British Standard EN-206 [50] that compressive strength for other sizes of samples should be estimated for non-representative values. Based on the above-mentioned discussion, in this project, the 100 × 200 mm cylinder strength was correlated to the paver block strength by performing laboratory tests. These results are presented later in this paper.

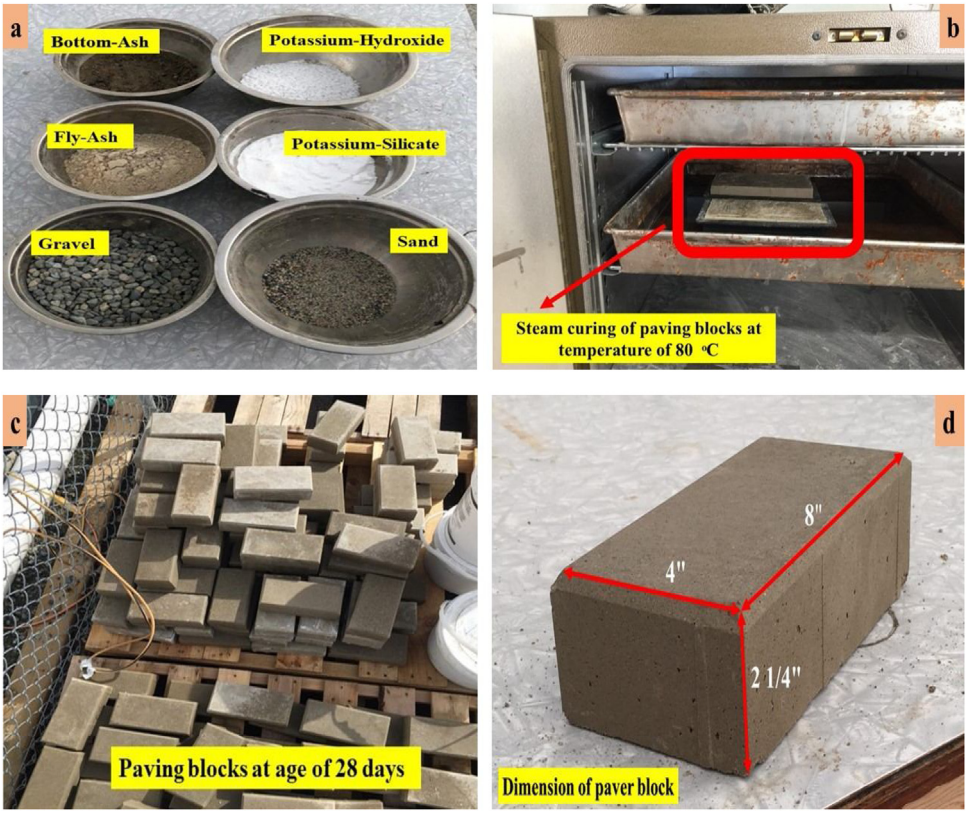

Fig. 4. Raw materials, curing temperature, shape and size of GPC.

5. Field placement details

Two areas at the entrance of parking lot#3 at the University of Victoria were selected to place a total of 150 GPC and 210 PCC paver blocks. Area 1 shown in Fig. 5(a) was designated to investigate the combined effect of traffic load and low temperature on properties of GPC and PCC. Fig. 5(b) (Area 2) indicates the designated area for studying the effect of low temperature only on the relative dynamic modulus of elasticity and leach-ability of GPC and PCC. Paver blocks in this section were not expected to be exposed to any traffic load.

Fig. 5(a) shows the placement area of 2.22×1 m^2 and 3×1 m^2 for GPC and PCC paver blocks respectively. Fig. 5(b) also indicates that the GPC and PCC placement size is 1×0.72m^2 and 1×1m^2 respectively. Traffic shown in Fig. 5(c) was expected to cross straight over the paver blocks and to turn over an existing concrete slab. So both paver types were exposed to more or less the same conditions.

6. Test methods

Initial testing on GPC cylindrical samples was performed during the mix optimization phase. As mentioned earlier, the highest compressive strength was achieved at a temperature of 80 °C of steam curing. So, samples for all subsequent tests were cured at a temperature of 80 °C. In this research, Non-Destructive Testing (NDT) devices such as rebound hammer and ultrasonic pulse velocity were also employed to evaluate the properties of GPC and PCC exposed to real environmental conditions.

6.1. Compressive strength of cylinders

A total of 54 GPC cylindrical samples (100 mm diameter and 200 mm height) were tested in accordance with ASTM C39 [51] using the Forney compression testing machine #AD 650. According to ASTM C39 [51], the compressive load on the specimen was applied at a rate of 0.25 ± 0.05 MPa/s.

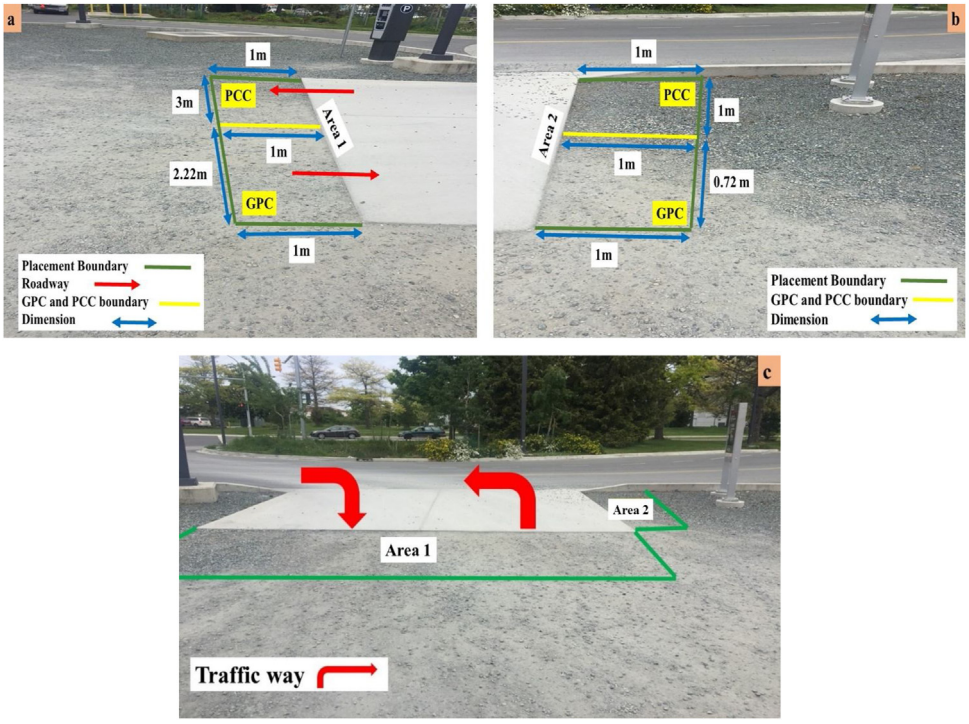

Fig. 5. Site details.
(a) Area for effect of low temperature & traffic load investigation.
(b) Area for low temperature, relative dynamic elastic modulus & leach-ability.
(c) Traffic way.

6.2. Compressive strength of paver blocks

According to ASTM C805 [52], Schmidt hammer or rebound hammer processes the rebound of a spring-loaded mass impacting against the surface of a concrete sample. The Schmidt hammer knocks the concrete surface at certain energy. Its rebound is dependent on the rigidity of the concrete surface/sample. The rebound rate can be used to measure the concrete's compressive strength by using a conversion chart. In this study, Original Proceq Schmidt hammer Type N/NR, as a surface hardness method, was used to measure the change in compressive strength of paver blocks every month after initial placement in accordance with ASTM C805 [52]. The tests can be carried out in three positions including horizontal, vertically (upward or downward) and angled position. In this study, Schmidt hammer was hit on the top surface of the paver blocks vertically downward to measure their in-place compressive strength. According to ASTM C805 [52], an average of ten Schmidt hammer readings was calculated to obtain accurate results. Moreover, Schmidt hammer was calibrated to be functioning properly after each thirty reading using an ideal test anvil.

6.3. Ultrasonic pulse velocity

UPV is one of the effective methods to determine uniformity and quality of concrete. The UPV method evaluates the travel time of longitudinal ultrasonic waves passing through the concrete. The path length between transducers divided by the travel time gives the average velocity of wave propagation. UPV is used to check the existence of internal flaws and voids in accordance with ASTM C597 [53]. Velocity reduction of UPV test results shows the internal deterioration of the specimens [54]. In this study, the Pundit Lab Proceq UPV test instrument was used with bandwidth, measuring resolution, pulse voltage UPV and nominal transducer frequency of 20–500 kHz, 0.1 us, 125–500 V and 24–500 kHz respectively. Indirect transmission method (transducers were held on the same surface) was used to evaluate the velocity of paver blocks in-situ. Since the paver blocks were placed on bedding sand and since UPV of sand is different from that of UPV of paver blocks, the optimum pulse width, length and height parameters in the device were set to the dimensions of paver blocks so as to only measure the UPV of paver blocks and eliminate any effect of its surroundings. Every month, three readings were recorded from each paver block to have accurate data of their UPV.

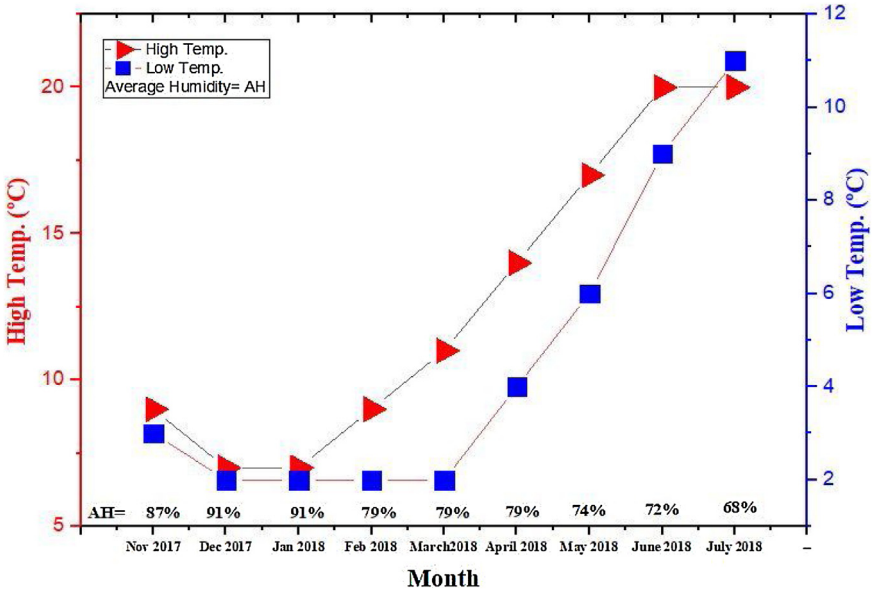

Fig. 6. Highest and lowest temperature over months [55].

The following equation was used to predict the dynamic modulus of elasticity form measured UPV in accordance with ASTM C597 [53]:

$$E = \frac{\boldsymbol{\rho}\ (1+\boldsymbol{\mu})(1-2\boldsymbol{\mu})\mathbf{V}^2}{1-\mu} \tag{1}$$

E = dynamic elastic modulus, GPa

ρ = density in kg/m^3 (Average measured density of GPC: ρ_{GPC} = 2439 kg/m^3 and average assumed density of PCC: ρ_{PCC}=2400 kg/ m^3)

V = measured pulse velocity in m/second

μ= assumed dynamic Poisson's ratio (μ = 0.24 for both types of concrete)

6.3.1. Seasonal humidity effects

The humidity of materials changes their response to ultrasonic waves passing through them. Hence, it is important to investigate the effect of seasonal humidity on the velocity of paver blocks since the paver blocks are exposed to wetting-drying cycles and different humidity conditions. Generally, in the field, all the paver blocks experienced three humidity conditions: fully wet, Saturated Surface Dry (SSD) and dry. So, the same laboratory conditions were simulated to measure the effect of humidity on velocity and compressive strength of paver blocks. These results are reported later. Fig. 6 shows the average of high and low temperatures and average humidity recorded in the city of Victoria from November 2017 to August 2018 [55]. The Schmidt hammer and UPV test were performed over 240 days with the lowest and highest temperatures of 1 °C–20 °C respectively. These results are also reported later.

6.4. Resonant frequency test

Resonant Frequency Test (RFT) or Resonant Frequency Gauge (RTG) as a new NDT method has brought a lot of attention to determine material deterioration. However, this method is typically only performed in a lab environment. While, UPV method can be used either on-site or in the laboratory. So, a comparison between relative dynamic modulus of elasticity based on RFT and UPV was made to develop a better understanding of any correlation that exists between these two methods. RFT/RTG method is based on the determination of fundamental transverse, longitudinal and torsional resonant frequencies of vibration of a concrete sample that is created by an impact and sensed by an accelerometer.

Fig. 7 shows different parts of the RTG/RFT device which is designed for laboratory usage. Transverse impact RFT and UPV test were performed on thirty paver blocks (in the lab) to measure the dynamic modulus of elasticity. In this study, Olson RFT/RTG instrument consists of a USB powered RTG device, BNC connection, 2 oz. ball-peen hammer (spherical head hammer), an accelerometer (10 mV/g) and Windows 7–10 device running Olson instruments' RFT/RTG software were used. The following equation was used to predict the dynamic modulus of elasticity in accordance with ASTM C215 [56]:

$$Gd = CMn^2 \tag{2}$$

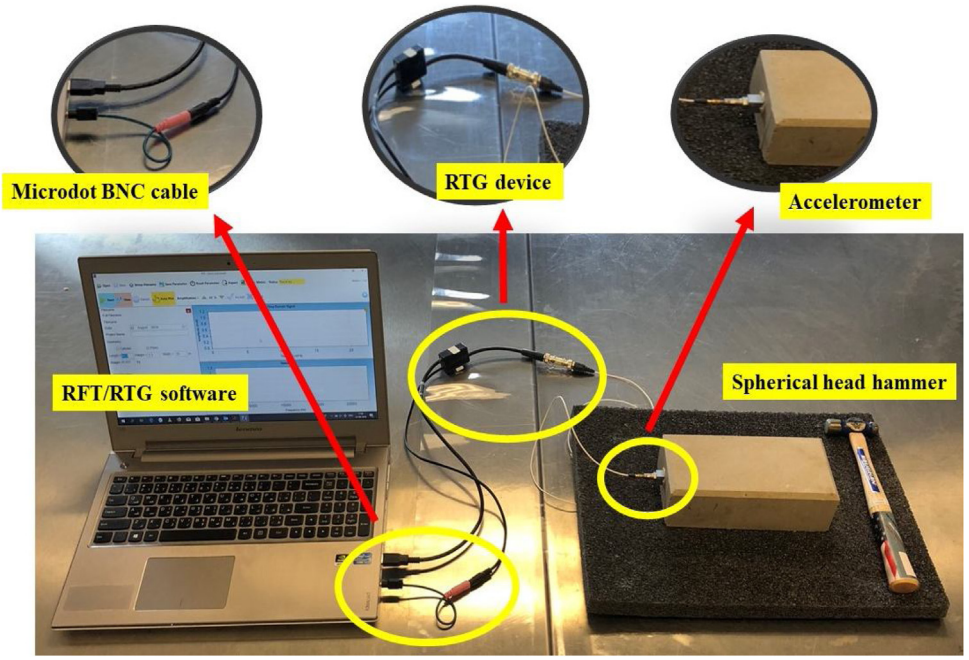

Fig. 7. The main components of RTG/RFT equipment.

Where

Gd = dynamic elastic modulus, GPa,
C = 0.9464 (L^3T/bt^3), m^{-1},
L = length of GPC prism, m,
M = mass of GPC cylinder (kg),
N = fundamental transverse frequency, Hz,
t, b = dimensions of cross-section of a prism, m,
T = correction factor

6.5. Water quality assessment

Chemical activators and waste materials contain heavy metals that can be mobilized and can leach into the environment [57]. Hence, the leach-ability of GPC and PCC paver blocks were measured to trace metals in accordance with the United States Environmental Protection Agency Standard 1311 [58]. The leaching tests were performed using HACH strips to determine the quality of collected sample water from the site.

7. Results and discussions

7.1. Laboratory investigation of GPC and PCC samples

7.1.1. Compressive strength of cylindrical GPC samples

Dissolution and geopolymerization of alumina-silicate gel of GPC significantly depend on the curing condition. Both higher curing temperature and duration can be used to accelerate the polycondensation process [59,60]. Steam curing and dry curing methods were used to accelerate curing of GPC at five different temperatures including ambient, 30 °C, 45 °C, 60 °C, 80 °C. As can be seen in the Fig.8, highest compressive strength was achieved at a temperature of 80 °C of steam curing. It was also observed that the compressive strength of steam-cured samples and dry-cured samples increased by about 3.5 and 2.3 times respectively when the curing temperature was changed from ambient temperature (≈ 10 °C) to 80 °C. Fig. 8 also shows that for the type of GPC developed in this study, a minimum increase in strength is realized when curing temperature is increased from ambient to 30 °C. Compressive strength almost doubles when GPC is steam-cured at 45 °C as opposed to 10 °C. At all temperatures, steam curing outperforms dry curing. The authors attribute this to full and uniform internal curing of steam-cured samples. This study also indicates that reasonable strength can be achieved at 60 °C of curing and for some applications it may not be necessary to cure at high temperatures such as 80 °C. However, the target compressive strength of 35 MPa for the current application/construction area (parking lot with light traffic) was achieved at 80 °C after initial trial experiments on GPC samples. The abovementioned finding is in good-agreement with a performed study by Noushini et al.

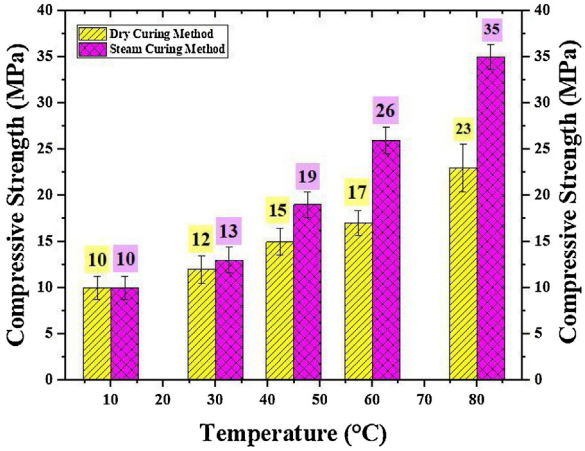

Fig. 8. Average compressive strength of steam-cured and dry-cured GPC samples.

[61] that Na-based GPC made only with fly-ash achieved a higher rate of compressive strength ranged from 27.4 to 62.3 MPa when samples were exposed to elevated temperature (23−90 °C). However, it should be noted that Na-based GPC made only with fly-ash slightly reached to higher compressive strength than K-based GPC made by fly-ash and bottom-ash (present study) cured to the same temperature and duration. It can be attributed to lower activation potential of KOH compared to NaOH which is because of the ionic diameter difference between sodium and potassium [62].

7.1.2. Compressive strength of both GPC and PCC paver blocks

Six paver blocks were cast and later cured at a temperature of 80 °C to find the compressive strength ratio between rectangular-shaped and cylindrical-shaped specimens. The samples were placed horizontally between two plates of the compressive testing machine. As can be seen in Fig. 9, the GPC paver block samples give an average compressive strength slightly lower than the cylindrical samples with the same curing method possibly due to higher stress concentration at corners of paver blocks [63]. This result shows that British Standard EN-206 [50] overestimated the compressive strength of the GPC paver block. One reason for this discrepancy can be attributed to the fact that this standard was originally designed for calculating the compressive strength of PCC and not GPC.

The average compressive strength and geometry conversion factor of GPC paver blocks were about 31.4 MPa and 0.89 respectively. The average compressive strength of PCC paver blocks was 33.5 MPa. No conversion factor for PCC paver blocks could be calculated as commercially available PCC paver blocks were used and no cylinders could be cast. However, it is reported by Ngoc et al. [64] that the mean compressive strength conversion factor of cubic samples (size 150 mm) and cylindrical compressive strength (150 × 300 mm) is 0.84.

7.1.3. Effect of humidity on mass and velocity of GPC and PCC

According to ASTM C597 [53], the humidity level of concrete samples affect the pulse velocity. Laboratory simulation of seasonal conditions was performed to measure the mass and velocity of paver blocks at different humidity levels to have a

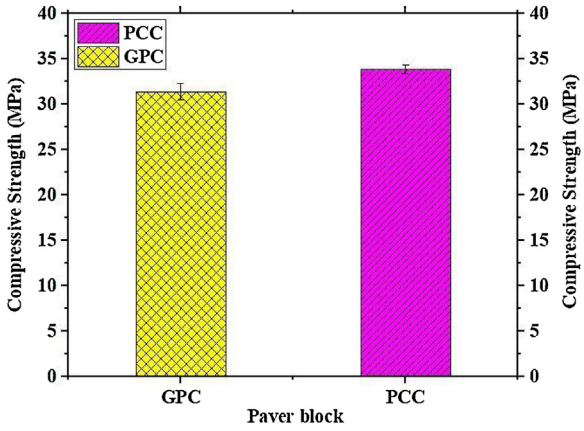

Fig. 9. Average compressive strength of GPC and PCC paver blocks.

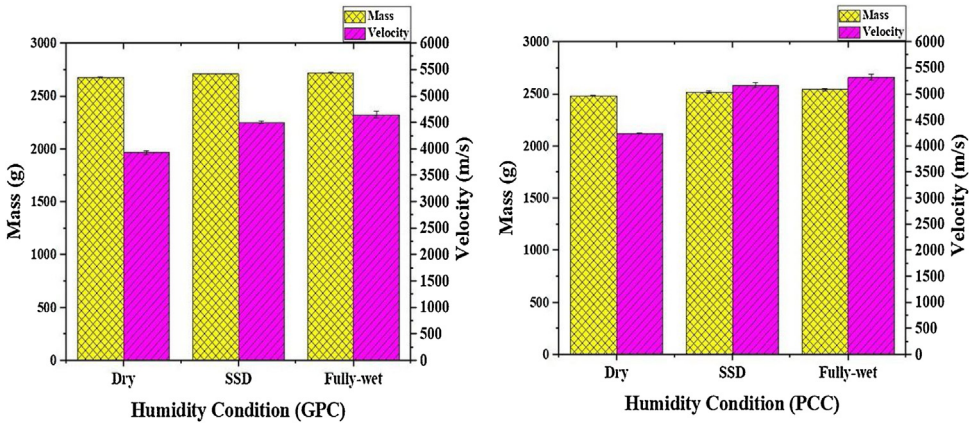

Fig. 10. Effect of humidity on mass and velocity of GPC and PCC.

better understanding of the effect of humidity and wetting-drying cycles on the velocity of paver blocks in real environmental conditions. Six GPC and PCC paver blocks were immersed into water to measure the mass and UPV of SSD and fully wet samples (soaked for 14 days).

Fig.10 shows the average mass and velocity of GPC and PCC paver blocks in three humidity conditions. The GPC samples showed that the mass and velocity ratio between dry and fully wet conditions is about 0.98 and 0.84 respectively. While, it can be observed from the results of PCC samples that the mass and velocity ratio between dry and fully wet conditions is about 0.97 and 0.79 respectively. So, for both types of concrete, the velocity and mass increased with a higher humidity level as would be expected. It is also noted that the susceptibility for mass and velocity to increase with an increase in moisture was similar for both types of concrete.

7.2. On-site compressive strength and velocity

Fig. 11 is a schematic showing the placement of PCC and GPC paver blocks on-site. In area 1, codes 1–8 are for GPC and codes 9–22 are for PCC paver blocks. In area 2, codes 1–3 are for GPC and codes 4–8 are for PCC paver blocks. The codes/numbers are later used as labels in Figs. 12 and 13. The total number of paver block rows for GPC and PCC are shown with red color and blue color respectively. Three rows shown with green hatch were considered just for investigation of the effect of traffic load but it is beyond the scope of this paper.

The relationship between compressive strength, average velocities of each GPC and PCC paver blocks are shown in Figs. 12 and 13. The compressive strength and velocity of paver blocks were measured every month after the initial placement.

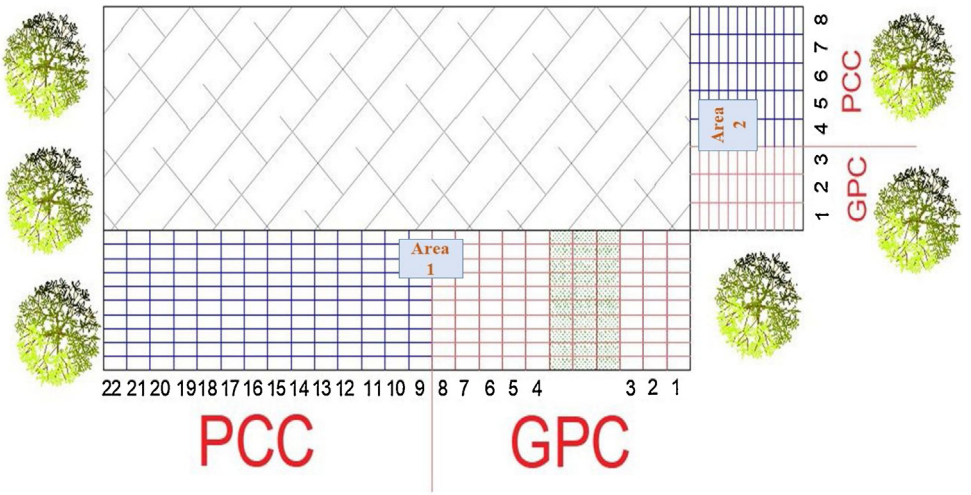

Fig. 11. Top view of sites and coding pattern.

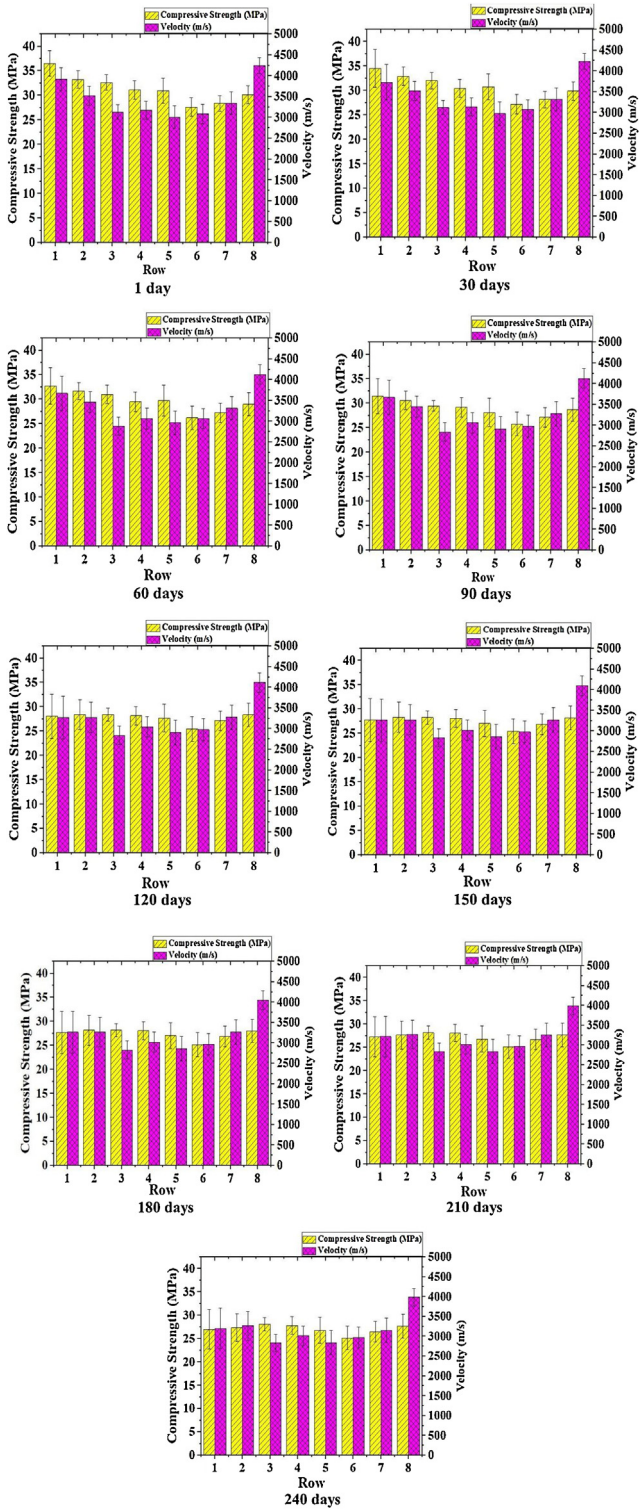

Fig. 12. Average compressive strength and velocity of paver blocks over 240 days of exposure (1-8 rows).

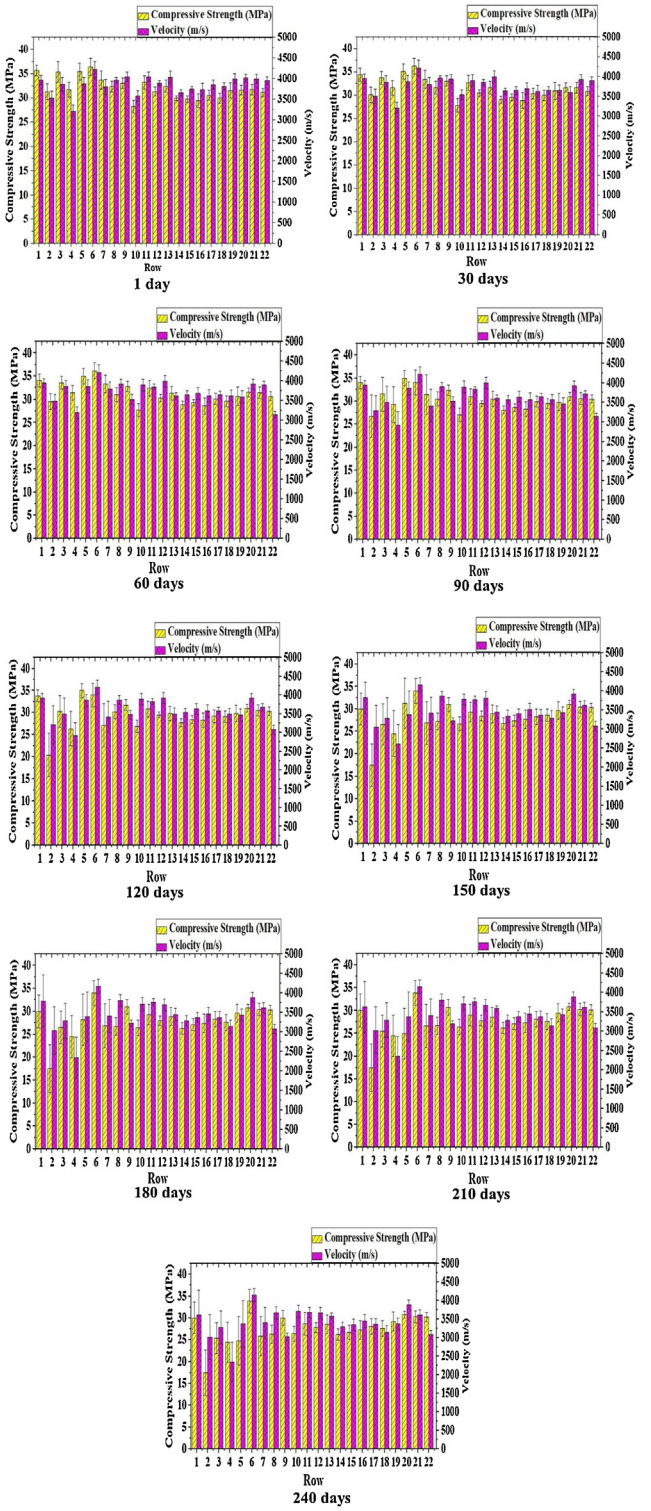

Fig. 13. Average compressive strength and velocity of paver blocks over 240 days of exposure (1-22 rows).

7.2.1. Compressive strength and velocity of GPC

From visual inspection, over the first 60 days, small local deterioration of surface (scaling) of some GPC paver blocks was observed. This action led to large cracks extending downward from the damaged zone to the bottom of GPC paver blocks (15 blocks). Over the following 60 days, more voids were available for organic and inorganic solutions to permeate through the

GPC paver blocks and produce more spalling in GPC paver blocks. After 120 days of exposure to real environmental conditions, the compressive strength and velocity decreased and finally, after approximately 240 days, 15 % of GPC paver blocks showed reduced strength and velocity and consequently, their testing was terminated. Of the total placed, 85 % of paver blocks indicated acceptable results.

In this study, attempts were made to take all readings of UPV and compressive strength on a single day to minimize the effect of changing environmental factors. Fig. 12 shows average compressive strength and velocity of 35 GPC and 59 PCC paver blocks and Fig. 13 shows average compressive strength and velocity of 80 GPC and 140 PCC paver blocks.

Both Figs. 12 and 13 show the change in average compressive strength and velocity of paver blocks over 240 days of exposure. As can be seen in Figs. 12 and 13, on an average, the compressive strength and velocity of GPC paver blocks were higher than PCC paver blocks on the first day of experiments compared to 150 days of exposure; compressive strength and velocity of GPC decreased progressively over 150 days of exposure. However, it can also be seen that the compressive strength and velocity of both types of paver blocks decreased slightly from 150 days to 240 days of exposure.

Fig. 12 shows that when the age of exposure increased from 1 to 240 days, the average velocity of GPC paver blocks (1–3) decreased from 3523.2–3099.3 GPa whereas the average velocity of PCC (4–8) paver blocks decreased from 3370.8–3192.8 GPa. It also can be seen in Fig. 12 that the average compressive strength of GPC (1–3) and PCC (4–8) decreased by 19.51 % and 9.65 % respectively.

Fig. 13 indicates that the average velocity of GPC (1–8) and PCC (9–22) decreased about 11.6 % and 8.3 % respectively when the age of exposure increases from 1 day to 240 days. The average compressive strength of GPC (1–8) and PCC (9–22) also decreased about 23.4 % and 8.2 % over total age of exposure.

According to the American Concrete Institute (ACI) Code 318 [65], the paste content is interrelated to maximum aggregate size. So, GPC paste with small aggregate size desires more amount of AEA. Hence, the authors hypothesize that the scaling of damaged GPC paver blocks was due to an inadequate amount of AEA in the paste.

Permeability is another cause of scaling of concrete subjected to frost action. Although, GPC tends to show a greater permeability resistance than PCC [66], this does not mean low moisture absorption [67]. The general absence of micro-cracks in the Interfacial Transition Zone (ITZ) is the principal reason for low permeability [67]. As can be seen in Fig. 14, GPC paver blocks absorbed more water than PCC paver blocks. So, this could be another possible reason that GPC blocks experienced scaling phenomena. This finding is in good-agreement with a performed study by Albitar et al. [68] that the cement-based concrete has lower water absorption and sorptivity than fly-ash based and slag-based GPC due to the capillary mechanism of the pastes.

According to a performed study by Khater et al. [60], the curing regime is critical for the geopolymerization process of aluminosilicate gel which causes high early strength gain. However, heat-treatment must be applied in a proper way that it makes a supreme condition for the dissolution and precipitation of dissolved silica and alumina species. Overall, in this study, the visual inspection showed that another possible reason for GPC deterioration is shorter curing duration for the paver blocks during the manufacturing stage.

Three pits shown with red color (Fig. 14) were considered for collecting water samples permeated through paver blocks and estimating the leach-ability of GPC and PCC.

7.2.2. Compressive strength and velocity of PCC

In this study, the initial average reading of compressive strength and velocity of PCC showed lower values than GPC paver blocks. Although, contrary to common belief, the low compressive strength of concrete does not always lead to low durability. Basically, each 1 % of adding AEA in matrix decreases the strength of concrete by approximately 5 % [67] and as it is reported [67], non-air entrained concrete with higher strength may show lower frost resistance compared to air entrained concrete due to extra air voids provided to decrease the hydraulic pressure during exposure to low temperature. Moreover, it is reported by Levy et al. [69] that uniformly distribution of air bubbles/AEA through cement paste increases the freeze-thaw

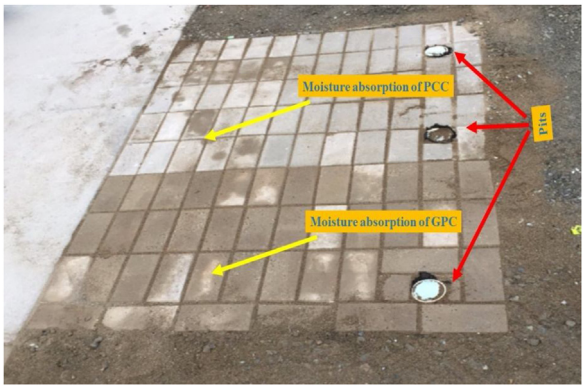

Fig. 14. Rate of moisture absorption of GPC and PCC paver blocks.

resistance of concrete. So, it can be concluded that a sufficient amount of AEA was added to the PCC matrix. Hence, this is one of the reasons that scaling phenomena was not observed on the surface of PCC paver blocks.

7.2.3. Leach-ability of GPC and PCC paver blocks

A healthy ecosystem and clean environments are essential to the survival of mankind and other organisms. Leaching assessment of materials made by waste by-products is vital to characterize the leaching potential of toxic metals. In this research, water-proof sheet membranes were used in the foundation of a section of paver blocks to prevent penetration of water to the sub-grade level and allow sampling of water that has percolated through the paver blocks and has been in contact with them. Water samples permeated through paver blocks were collected into three pits (Fig.14) to trace the total alkalinity, total hardness, pH, total chlorine, phosphate, copper, ammonia, iron, nitrate and nitrite. Every thirty days, six water samples were collected from each GPC and PCC pits. Fig. 15 shows that the pH of GPC and PCC is 7.9 and 6.8 respectively and these values were constant over the total age of exposure. GPC paver blocks show higher pH values than PCC which is attributable to the use of KOH [29]. This finding is in good-agreement with a performed study by Poursaee et al. [70] that Na-based GPC made by slag has a higher pH than PCC due to the presence of alkaline solution in GPC mixture. Furthermore, as it is reported by Izquierdo et al. [71] that heat-treatment of GPC improves the matrix microstructure, decreases the porosity of concrete and decreases the leach-ability of the binder. So, it can be concluded that steam curing improved the microstructure of GPC paver blocks and reduced the amount of heavy metals in water samples.

Total hardness in water refers to the amount of dissolved calcium (Ca) and magnesium (Mg). Generally, water hardness concentration below 60 ppm is considered as soft; 60–120 ppm, moderately hard; 120–180 ppm, hard, and more than 180 ppm, very hard. Kozisek et al. [72] suggested the highest and lowest rate of Ca (40–80 mg/l) and Mg (20–30 mg/l) in drinking water and defined total hardness as the sum of Ca and Mg concentration of 2–4 mmol/L. The total hardness of GPC and PCC is 120 ppm and 180 ppm respectively over 150 days of exposure. Iron as one of the main chemical elements of GPC and PCC is 0.15 and 0.2 respectively over the total age of exposure. For both types of concrete, other elements such as chlorine, Nitrate and Nitrite were constant over 150 days and their leach-ability were below the detection limit. The results show that all the metals were immobilized effectively for both types of concretes. All the elements of K-based GPC paver blocks were constant over 150 days as the steam curing method was used to develop the paste structure [71], which is attributed to a full reaction of fly-ash and bottom-ash particles. This is also confirmed by Zhang et al. [73] that slag-based GPC cured at 80 °C for 8 h can effectively immobilize chemical metals when the amount of chemical metals is in the range of 0.1–0.3 %.

7.3. Dynamic elastic modulus

7.3.1. Comparison between dynamic elastic modulus of RFT and UPV

In this study, after 180 days of exposure, thirty paver blocks were extracted from the site to make a comparison between relative dynamic elastic modulus derived from UPV and RFT.

Average dynamic modulus of elasticity derived from RFT and UPV were calculated in accordance with ASTM C215 [56] and ASTM C597 [53] respectively. In this study, the UPV and the transverse resonant frequency of GPC paver blocks were converted to relative dynamic elastic modulus using Eqs. (1) and (2) respectively. At zero days of exposure, the average relative dynamic elastic moduli from RFT and UPV was 12.20 GPa and 7.78 GPa respectively. A comparison between dynamic elastic moduli of GPC [37] and reported dynamic elastic moduli for PCC [67] shows that GPC has lower values than PCC. Basically, dynamic elastic moduli of concrete is improved by the modulus of elasticity of the raw constituents, aggregate porosity, properties of paste and characteristics of transition zones such as capillary voids and micro-cracks [67]. The abovementioned finding is confirmed by Fang et al. [74] that due to the various factors including slag replacement level, amount of molarity etc., the dynamic elastic modulus of GPC made by fly-ash and slag is varied from 12 to 58 GPa.

Initially, average relative dynamic elastic moduli of GPC paver blocks before exposure to cold weather was considered to be 100 % to have a unique reference and then the average relative dynamic elastic moduli of GPC after 180 days of exposure was calculated and was expressed in percentage to determine material deterioration using the two NDTs.

As can be seen in Fig. 16, relative dynamic elastic modulus decreased after 180 days of exposure. It can also be observed that the relative dynamic elastic modulus calculated using the RFT method is higher than that obtained from the UPV method. This difference between the relative dynamic elastic moduli of RFT and UPV can be due to surface conditions among other reasons. About 18 pavers blocks had uneven surface after 180 days of exposure and basically, smoothness of contact the surface affects UPV [75]. While, RFT can measures frequency even on a bumpy surface.

7.3.2. Dynamic modulus of elasticity of GPC and PCC paver blocks

Table 8 shows the average relative dynamic modulus of elasticity of GPC and PCC paver blocks placed in area 2. This was calculated using UPV values. As can be seen, the relative dynamic modulus of elasticity of PCC is higher than that of GPC paver blocks over the entire test period. The relative dynamic modulus of elasticity decreased progressively in the first two months of exposure for both types of concretes. However, test results reveal that after two months, the dynamic elastic modulus of GPC paver blocks decreased much faster than that of PCC.

Yawei et al. [76] established a damage mechanism model by using relative dynamic elastic modulus and proposed that a power function model is more precise than an exponential function model. The same models were used to create a dynamic elastic modulus attenuation model for both types of paver blocks under real environmental conditions.

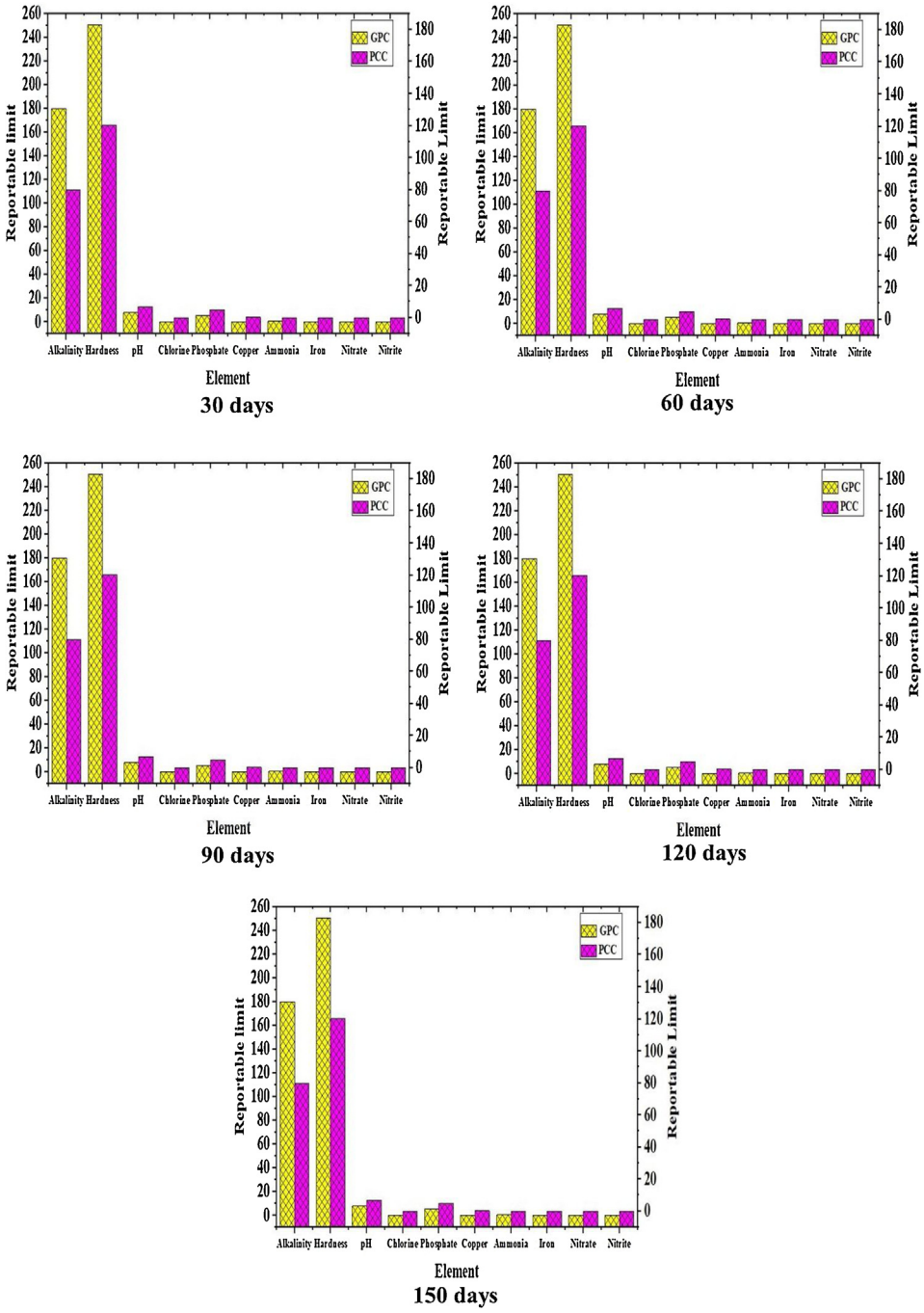

Fig. 15. Leach-ability of chemical elements of GPC and PCC over 150 days of exposure.

Yawei et al. [76] assumed that E_0 is the initial dynamic modulus of elasticity of samples and E_n is the dynamic modulus of elasticity after N number of freeze-thaw cycles. In our study, N was considered as exposure period (N = 1 for every 30 days) since the temperature variation was not controllable in real environmental conditions. According to the exponential function, relative dynamic elastic modulus attenuation can be created as:

$$Y = E_n/E_0 = ae^{bN} \tag{3}$$

$$E_n = E_0\, ae^{bN} \tag{4}$$

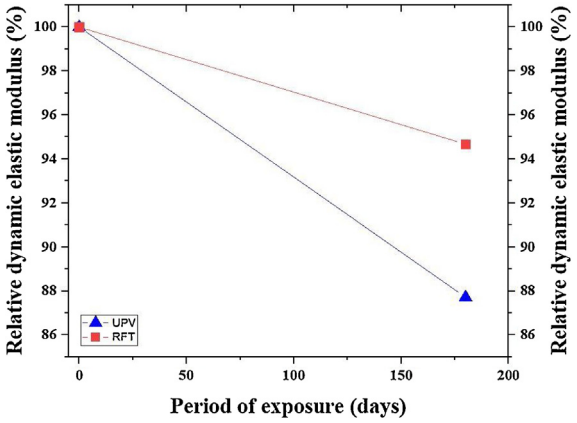

Fig. 16. Relative dynamic modulus of elasticity of UPV vs. RFT.

Table 8
Relative dynamic elastic modulus of GPC and PCC over 240 days of exposure.

Exposed (Days)	GPC Relative dynamic elastic modulus (%)	PCC Relative dynamic elastic modulus (%)
1	100	100
30	98.04	99.04
60	94.83	97.93
90	94.28	96.5
120	91.20	96.18
150	88.70	95.54
180	88.56	95.38
210	88.14	95.23
240	85.49	95.23

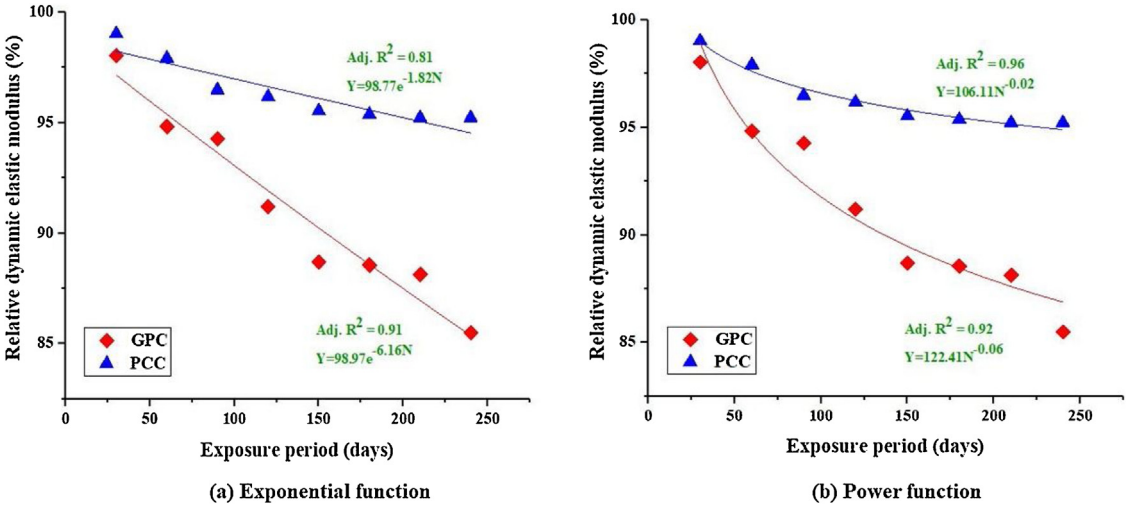

Fig. 17. Comparison between exponential and power function.

The power model also can be used to create a relative dynamic elasticity modulus model:

$$Y = E_i/E_0 = aN^b \quad (5)$$

Where,

Y = Relative dynamic elasticity modulus of samples, percentage

E_n and E_i= Dynamic elasticity modulus of samples after N times freeze-thaw cycles, percentage

E_0= Dynamic elasticity modulus of samples before exposing to freeze-thaw cycles, percentage

a and b = Constant variables

The Eqs. (4) and (5) were modeled in Origin software to establish a damage model for both types of concrete used in this study and are plotted in Fig. 17(a) and (b) respectively. The values from the models are plotted alongside measured field data (shown in Table 8).

According to the power function, the coefficients a and b for GPC were 122.41 and -0.06 respectively. While, the coefficients a and b for PCC were 106.11 and -0.02 respectively. It also can be observed from figures that Adj.R^2 of power function of both GPC and PCC is superior compared to the exponential function. Hence, this function can be used to correlate field exposure to damage of GPC and PCC as it has fewer errors. It should, however, be noted that this proposed model is valid for the somewhat mild winter conditions recorded in Victoria, Canada. Hence, caution should be exercised before using this model to paver blocks in more severe weather conditions.

8. Conclusions

The objectives of this study were to investigate the effect of real environmental exposure on leach-ability and change in mechanical properties of K-based GPC. This was further compared to traditional concrete (PCC). Numerous conclusions can be drawn from the present study:

- Steam curing and dry curing methods increase the compressive strength of GPC by about 3.5 and 2.3 times respectively when the temperature increases from ambient temperature (-10 °C) to 80 °C. The compressive strength of steam-cured GPC was higher due to the prevention of excessive moisture evaporation, and due to the identical internal curing of GPC samples.
- According to the results of compression test on rectangular and cylindrical GPC samples, rectangular steam-cured GPC samples showed an average compressive strength lower (about 10.28 %) than the cylindrical steam-cured GPC samples probably because of the higher rate of stress concentration at corners of rectangular steam-cured GPC samples. The average strength conversion factor between cylindrical and rectangular GPC samples is 0.89.
- The laboratory simulation of seasonal humidity was also carried out to measure the effect of moisture level (dry, SSD, fully wet) on mass and UPV of both GPC and PCC. The results of the experiment indicate that the velocity and mass of GPC and PCC samples increased when humidity level was changed from dry condition to fully wet condition. The mass and velocity ratio of GPC was about 0.98 and 0.84 respectively when the moisture level were increased from dry to fully wet. Whereas, the mass and velocity ratio of PCC samples was 0.97 and 0.79 respectively.
- According to the results of the UPV test, the decrease in velocity of GPC was about 11.6 % (area 1) and 12.03 % (area 2). While, the velocity of PCC decreased about 8.3 % (area 1) and 5.28 % (area 2). Moreover, the result of the Schmidt hammer showed that the average compressive strength of GPC decreased about 2.34 % (area 1) and 19.51 % (area 2). Whereas, the decrease in compressive strength of PCC was about 8.2 % (area 1) and 9.65 % (area 2).
- The leach-ability of heavy metals, including total alkalinity, total hardness, pH, total chlorine, phosphate, copper, ammonia, iron, nitrate and nitrite of PCC and GPC paver blocks were measured every thirty days (150 days in total) of exposure to real environmental conditions using HACH strips. The results show that the pH of GPC paver blocks is 13.92 % higher than pH of PCC paver blocks due to the use of KOH in the GPC paver block mixture. The results also indicated that the steam curing method helped GPC to develop paste structure and caused all the chemical metals of GPC paver blocks to remain constant over 150 days of exposure.
- The relative dynamic modulus of elasticity was correlated to the field exposure of paver blocks. In this regard, a damage mechanism model was derived for both PCC and GPC paver blocks after 240 days of exposure to real environmental conditions using the power functional model and exponential function model. The comparison between exponential and power function showed that power function is superior to exponential function due to the higher achieved values of Adj.R^2 for both GPC (0.96) and PCC (0.92).

9. Challenges

In developing GPC, the chemical component of precursors including the chemistry phase and size of particles is critical in the reaction process with alkaline solutions. High quality-checking and optimization of coal ashes and activators are always required to make high-quality GPC as the different type of by-product materials are available in various power plants.

Basically, GPC certainly is a sensitive material to temperature and humidity compared to PCC. So, more facilities such as steam curing oven, skills and expertise are required to cure fresh paste in either real environmental conditions or at the laboratory.

Despite the growing market pull for ‘sustainable’ construction materials, such a technology is not available on an industry-wide level and has restricted applications in the market. Consequently, there are no related standards for GPC reported up to date and basically, standards made for PCC are used for performing tests on GPC.

The curing regime of GPC is another concern in the cold region due to GPC’s sensitivity to moisture and temperature. So, in-situ curing in such cold conditions needs more heat for realizing full strength.

Declaration of Competing Interest

None.

Acknowledgements

The authors appreciatively acknowledge the financial support from Canada-India Research Centre of Excellence (IC-IMPACTS) and authors are also thankful to Dr. Urmil Dave, Professor at Nirma University, for his help in this study; Matt Dalkie, technical services engineer of Lafarge Canada Inc. and Mike McDonald, field chemist of National Silicates an affiliate of PQ Corporation Company for providing materials for this study. Authors also like to thank Priyanka Morla for her help in production of GPC paver blocks.

References

[1] N.H.A.S. Lim, H. Mohammadhosseini, M.M. Tahir, M. Samadi, A.R.M. Sam, Microstructure and strength properties of mortar containing waste ceramic nanoparticles, Arab. J. Sci. Eng. 43 (10) (2018) 5305–5313.
[2] H. Mohammadhosseini, N.H.A.S. Lim, M.M.T.R. Alyousef, H. Alabduljabbar, M. Samadi, Enhanced performance of green mortar comprising high volume of ceramic waste in aggressive environments, Constr. Build. Mater. 212 (2019) 607–617.
[3] G. Dimitriou, P. Savva, M. Petrou, Enhancing mechanical and durability properties of recycled aggregate concrete, Constr. Build. Mater. 158 (2018) 228–235.
[4] H. Mohammadhosseini, A. Abdul, H.E. Abdul, Influence of palm oil fuel ash on fresh and mechanical properties of self-compacting concrete, Indian Acad. Sci. 40 (2015) 1989–1999.
[5] F. Okoye, Geopolymer binder: a veritable alternative to Portland cement, Materialstoday: Proceed. 4 (4) (2017) 5599–5604.
[6] B. Singh, I.G.M. Gupta, S. Bhattacharyya, Geopolymer concrete: a review of some recent developments, Constr. Build. Mater. 85 (2015) 78–90.
[7] H. Hardjasaputra, M. Cornelia, Y. Gunawan, I. Surjaputra, H. Lie, Rachmansyah, G.P. Ng, Study of mechanical properties of fly ash-based geopolymer, IOP Conf. Ser.: Mater. Sci. Eng. 615 (2019)012009.
[8] L.M. Zerzouri, S. Alehyen, M.E. Alouani, M. Taibi, The effect of aggressive environments on the properties of a low calcium fly ash based geopolymer and the ordinary Portland cement pastes, Mater. Today. Proc. 13 (2019) 1169–1177.
[9] D.Sd.T. Pereira, F.J. daSilva, A.B.R. Porto, V.S. Candido, A.C.R. daSilva, F.D.C.G. Filho, S.N. Monteiro, Comparative analysis between properties and microstructures of geopolymeric concrete and portland concrete, J. Mater. Res. Technol. 7 (2018) 606–611.
[10] F. Nabeel, M. NeazSheik, M. N.S.Hadi, Investigation of engineering properties of normal and high strength fly ash based geopolymer and alkali-activated slag concrete compared to ordinary Portland cement concrete, Constr. Build. Mater. 196 (2019) 26–42.
[11] Y. Abualrous, Characterization of Indian and Canadian Fly Ash for Use in Concrete, Department of Civil Engineering, University of Toronto, Toronto, Canada, 2017.
[12] J. G.Speight, Chemicals in the environment, Reaction Mechanisms in Environmental Engineering, Butterworth-Heinemann, 2018, pp. 43–79.
[13] J. Thaarrini, V. Ramasamy, Feasibility studies on compressive strength of Ground coal ash geopolymer mortar, Periodica Polytechnica (Civil Engineering) 59 (2015) 373–379.
[14] Eu. Haq, S.K. Padmanabhan, A. Licciulli, Synthesis and characteristics of fly ash and bottom ash based geopolymers–a comparative study, Ceramic Int. 40 (2) (2014) 2965–2971.
[15] F. Okoye, J. Durgaprasad, N. Singh, Fly ash/Kaolin based geopolymer green concretes and their mechanical properties, Data Brief 5 (2015) 739–744.
[16] P. Chindaprasirt, C. Jaturapitakkul, W. Chalee, U. Rattanasak, Comparative study on the characteristics of fly ash and bottom ash geopolymers, Waste Manage. (Oxford) 29 (2) (2009) 539–543.
[17] R.M. Hamidi, Z. Man, K.A. Azizli, Concentration of NaOH and the effect on the properties of fly ash based geopolymer, Procedia Eng. 148 (2016) 189–193.
[18] F. Puertas, B. González-Fonteboa, I. González-Taboada, M.M. Alonso, M. Torres-Carrasco, G. Rojo, F. Martínez-Abella, Alkali-activated slag concrete: fresh and hardened behaviour, Cem. Concr. Compos. 85 (2018) 22–31.
[19] K. Sakkas, D. Panias, P.P. Nomikos, A.I. Sofiano, Potassium based geopolymer for passive fire protection of concrete tunnels linings, Tunnel. Underground Space Technol. 43 (2014) 148–156.
[20] A. Hosan, Sharany Haque, F. Shaikh, Comparative Study of Sodium and Potassium Based Fly-Ash Geopolymer at Elevated Temperature Australia, (2015) .
[21] D. Sabitha, J.K. Dattatreya, N. Sakthivel, M. Bhuvaneshwari, S.A.J. Sathik, Reactivity, workability and strength of potassium versus sodium-activated high volume fly ash-based geopolymers, Curr. Sci. 103 (2012) 1320–1327.
[22] T. Bakharev, Geopolymeric materials prepared using class F fly ash and elevated temperature curing, Cement Concrete 35 (6) (2005) 1224–1232.
[23] R. Siddique, Utilization of industrial By-products in concrete, Procedia Eng. 95 (2014) 335–347.
[24] T. Xie, T. Ozbakkaloglu, Behavior of low-calcium fly and bottom ash-based geopolymer concrete cured at ambient temperature, Ceram. Int. 41 (2015) 5945–5958.
[25] Y.P. Khandol, D.U. Dave, Development of Fly-Ash and Bottom-Ash Based Alkali Activated Paver Blocks, Department of civil engineering, institute of technology, Nirma University, Ahmedabad, 2016 382481.
[26] S.R. Hillier, C.M. Sangha, B.A. Plunkett, P.J. Walden, Long-term leaching of toxic trace metals from Portland cement concrete, Cem. Concr. Res. 29 (1999) 515–521.
[27] H. Lu, F. Wei, J. Tang, J. P.Giesy, Leaching of metals from cement under simulated environmental conditions, J. Environ. Manage. 169 (2016) 319–327.
[28] A.P. Galvín, F. Agrela, J. Ayuso, M.G. Beltrán, A. Barbudo, Leaching assessment of concrete made of recycled coarse aggregate: physical and environmental characterisation of aggregates and hardened concrete, Waste Manage. 34 (2014) 1693–1704.
[29] M. Izquierdo, X. Querol, J. Davidovits, D. Antenucci, H. Nugteren, C. Fernández-Pereira, Coal fly ash-slag-based geopolymers: microstructure and metal leaching, J. Hazard. Mater. 166 (2009) 561–566.
[30] A.S.T.M. C618/C618M, Standard Specification for Coal Fly Ash and Raw or Calcined Natural Pozzolan for Use in Concrete, American Society for Testing and Materials, USA, 2017.
[31] S. Pilehvar, V.D. Cao, A.M. Szczotok, M. Carmona, L. Valentini, M. Lanzón, R. Pamies, A.-L. Kjøniksen, Physical and mechanical properties of fly ash and slag geopolymer concrete containing different types of micro-encapsulated phase change materials, Constr. Build. Mater. 173 (2018) 28–39.
[32] R. Zhao, Y. Yuan, Z. Cheng, T. Wen, J. Li, F. Li, Z.J. Ma, Freeze-thaw resistance of class F fly ash-based geopolymer concrete, Constr. Build. Mater. 222 (2019) 474–483.
[33] Z. Yang, R. Mocadlo, M. Zhao, R. D Jr, M. Tao, J. Liang, Preparation of a geopolymer from red mud slurry and class F fly ash and its behavior at elevated temperatures, Constr. Build. Mater. 221 (2019) 308–317.
[34] F.-Y. Chang, M.-Y. Wey, Comparison of the characteristics of bottom and fly ashes generated from various incineration processes, J. Hazard. Mater. 138 (2006) 594–603.

[35] X. Goa, B. Yuan, Q. Yu, H. Brouwers, Characterization and application of municipal solid waste incineration(MSWI) bottom ash and waste granite powder in alkali activated slag, J. Cleaner Prod. 164 (2017) 410–419.
[36] R. Gupta, H.M. Rathod, Current state of K-based geopolymer cements cured at ambient temperature, Emerg. Mater. Res. 4 (1) (2015) 125–129.
[37] C. Yang, R. Gupta, Prediction of the compressive strength from resonant frequency for low-calcium fly ash-based geopolymer concrete, J. Mater. Civ. Eng. (2018) Vols. DOI:10.1061/(ASCE) MT. 1943-5533.0002228.
[38] F. Belforti, P. Azarsa, R. Gupta, U. Dave, Effect of Freeze-Thaw on K-Based Geopolymer Concrete and Portland Cement Concrete India, (2017) .
[39] IS 15658, Precast Concrete Blocks for Paving- Specification, Indian Standard, India, 2006.
[40] N. Ranjbar, C. Künzel, Cenospheres: a review," a review, Fuel J. 207 (2017) 1–12.
[41] F. Goodarzi, H. Sanei, Plerosphere and its role in reduction of emitted fine fly ash particles from pulverized, coal-fired power plants, Fuel J. 88 (2009) 382–386.
[42] R. Hooton, Bridging the gap between research and standards, Cem. Concr. Res. 38 (2007) 247–258.
[43] M.K. Wari, Bajpai, S. Dewangan, U. K, Fly ash utilization: a brief review in Indian context, Int. Res. J. Eng. Technol. (IRJET) 03 (04) (2016) 949–956.
[44] J. Davidovits, Geopolymer Chemistry and Application, 4 ed., Institut Geopolymere, France, 2015.
[45] P. Azarsa, R. Gupta, Novel approach to microscopic characterization of cryo formation in air voids of concrete, Micron 122 (2019) 21–27, doi:http://dx.doi.org/10.1016/j.micron.2019.04.004.
[46] ASTM C33/C33M, Standard Specification for Concrete Aggregates, American Society for Testing and Materials, USA, 2015.
[47] ASTM C192/C192M, Standard Practice for Making and Curing Concrete Test Specimens in the Laboratory, American Society for Testing and Materials, USA, 2015.
[48] N. Zabihi, Ö. Eren, Compressive strength conversion factors of concrete as affected by specimen shape and size," research journal of applied sciences, Eng. Technol. 7 (2014) 4251–4257.
[49] E. Ferretti, Shape-effect in the effective laws of Plain and rubberized concrete, CMC-Tech. Sci. Press 30 (2012) 237–284.
[50] EN 206, Concrete — Specification, Performance, Production and Conformity, British Standard, UK, 2014.
[51] ASTM C39/C39M, Standard Test Method for Compressive Strength of Cylindrical Concrete Specimens, American Society for Testing and Materials, USA, 2015.
[52] ASTM C805/805M, Standard Test Method for Rebound Number of Hardened Concrete, American Society for Testing and Materials, USA, 2013.
[53] ASTM C597/C597M, Standard Test Method for Pulse Velocity through Concrete, American Society for Testing and Materials, USA, 2016.
[54] S.A. Omer, R. Demirboga, W. H.Khushefati, Relationship between compressive strength and UPV of GGBFS based geopolymer mortars exposed to elevated temperatures, Constr. Build. Mater. 94 (2015) 189–195.
[55] AccuaWeather, AccuaWeather [Online]. Available:, (2017) . https://www.accuweather.com/en/ca/victoria/v8r/augustweather/47163?monyr=8/1/2018&view=table.
[56] ASTM C215/C215M, Standard Test Method for Fundamental Transverse, Longitudinal, and Torsional Resonant Frequencies of Concrete, American Society for Testing and Materials, USA, 2016.
[57] J.Z. Xu, Y.L. Zhou, Q. Chang, H.Q. Qu, Study on the factors of affecting the immobilization of heavy metals in fly ash-based geopolymers, Mater. Lett. 60 (2006) 820–822.
[58] USEPA, United States Environmental Protection Agency (US-EPA) Standard 1311, USEPA, USA, 2016.
[59] G.S. Ryu, Y.B. Lee, K.T. Koh, Y.S. Chung, The mechanical properties of fly ash-based geopolymer concrete with alkaline activators, Constr. Build. Mater. 47 (2013) 409–418.
[60] H. Khater, Effect of calcium on geopolymerization of aluminosilicate wastes, J. Mater. Civ. Eng. 24 (2011) pp. 902-101.
[61] A. Noushini, A. Castel, The effect of heat-curing on transport properties of low-calcium fly ash-based geopolymer concrete, Constr. Build. Mater. 112 (2016) 464–477.
[62] W.K. Part, M. Ramli, C.C. Ban, An overview on the influence of various factors on the properties of geopolymer concrete derived from industrial by-products, Constr. Build. Mater. 77 (2015) 370–395.
[63] M. Li, H. Hao, Y. Shi, Y. Hao, Specimen shape and size effects on the concrete compressive strength under static and dynamic tests, Constr. Build. Mater. 161 (2018) 84–93.
[64] L.T. Ngoc, C.-A. Graubner, Uncertainties of concrete parameters in shear capacity calculation of RC members without shear reinforcement, Beton- und Stahlbetonbau (2018) 1–8.
[65] ACI 318, Building Code Requirements for Structural Concrete and Commentary, American Concrete Institute, USA, 2014.
[66] K. Ramujee, M. Potharaju, Permeability and abrasion resistance of geopolymer concrete, Indian Concrete J. 88 (2014) 34–43.
[67] P.J.M. Monteiro, P.K. Mehta, Concrete Microstructure, 4 ed., Properties, and Materials, USA, 2014.
[68] M. Albitar, M.M. Ali, P. Visintin, M. Drechsler, Durability evaluation of geopolymer and conventional concretes, Constr. Build. Mater. 136 (2017) 374–385.
[69] S. Levy, Calculations relating to concrete and masonry, Construction Calculations Manual, (2012) , pp. 211–264.
[70] A. Poursaee, Corrosion of steel in concrete structures, Corrosion of Steel in Concrete Structures, (2016) pp. 139-33.
[71] M. Izquierdo, X. Querol, C. Phillipart, D. Antenucci, M. Towler, The role of open and closed curing conditions on The leaching properties of fly ash-slag-based geopolymer, J. Hazard. Mater. 176 (2010) 623–628.
[72] F. Kozisek, Health Risks from Drinking Deminirelized Water, Centre of Environmental Health, National Institute of Public Health, Prague, Czech Republic, 2004.
[73] Y. Zhang, S. Wei, C. Qianli, C. Lin, Synthesis and heavy metal immobilization behaviors of slag based geopolymer, J. Hazard. Mater. 143 (2007) 206–213.
[74] G. Fang, W.K. Ho, W. Tu, M. Zhang, Workability and mechanical properties of alkali-activated fly ash-slag concrete cured at ambient temperature, Constr. Build. Mater. 172 (2018) 476–487.
[75] Indian Standard 1331, Non-Destructive Testing of Concrete Methods of Test, Indian Standard, India, 2016.
[76] F. Yawei, L. Cai, Y. Wu, Freeze–thaw cycle test and damage mechanics models of alkali-activated slag concrete, Constr. Build. Mater. 25 (2011) 3144–3148.